Catalysis Letters Vol. 113, Nos. 1–2, January 2007 (© 2007)
DOI: 10.1007/s10562-006-9013-5

Pd–Al interaction at elevated temperatures: a TEM and SAED study

Simon Penner,* Bernd Jenewein, and K. Hayek

Institute of Physical Chemistry, University of Innsbruck, Innrain 52a, A-6020 Innsbruck, Austria

Received 29 September 2006; accepted 15 November 2006

Epitaxially grown Pd particles partly embedded in amorphous Al_2O_3 were subjected to annealing and reductive treatments in the temperature range 523–873 K to induce a possible Pd–Al interaction. The structural, morphological and compositional changes were monitored by transmission electron microscopy and selected area electron diffraction. Formation of Pd_4Al_3 and PdAl alloys has been observed upon annealing in 1 bar He for 1 h at $T > 523$ K and upon reduction in 1 bar H_2 for 1 h at $T \geq 523$ K, respectively. Both alloys appear to be stable up to 873 K, although Pd_4Al_3 shows beginning decomposition at and above 873 K. The stability under oxidative conditions was found to be very similar, a transformation back into metallic Pd sets in for both compounds at around 573–623 K. In agreement with previous studies on Pd/SiO_2, the formation of an amorphous hydride phase and/or a heavily distorted Pd lattice has been detected after reduction in hydrogen at 523 K.

KEY WORDS: Palladium; Al_2O_3; electron microscopy; selected area diffraction; alloying; Pd_4Al_3; PdAl; structural stability; reduction; annealing treatment.

1. Introduction

Alumina-supported palladium is not only an excellent catalyst for methane combustion and a promising catalyst for a variety of important oxidation reactions [1–5], but also exhibits high catalytic activity and selectivity in reforming reactions of alkanes [6–10]. Most notable in this respect is the high overall activity and isomerization selectivity of C_6 alkanes (*n*-hexane and 2,2-dimethylbutane) [6,7,9,10] and neopentane [8] after a high-temperature reduction in hydrogen at around 973 K. At least in part, this enhancement was reported being due to increased Pd–Al interaction at these high temperatures, resulting in Pd–Al alloys. It was also observed that the Pd–Al alloy decomposes during regeneration of the catalysts in oxygen, giving rise to a decreased catalytic activity [10]. Hence, the Pd–Al system acts like a typical SMSI system [11].

Pd–Al alloy formation has been observed upon depositing Pd on both polycrystalline Al surfaces [12,13], Al films [14,15] and Al(001) single crystals and has also been tackled by a variety of different methods, including X-ray photoelectron spectroscopy [12,13, 16,17], ion scattering [16,17], thermal desorption spectroscopy [12,13,17], secondary ion mass spectroscopy [12,17] and CO adsorption [12,13,17,18]. However, apart from sintering studies on Pd/Al_2O_3 catalysts [19], no detailed electron microscopic investigations of the interaction between Pd and Al have been carried out so far.

*To whom correspondence should be addressed.
E-mail: simon.penner@uibk.ac.at

We therefore aim at a detailed study of the Pd–Al interaction both under reductive and annealing conditions and of the subsequent structural stability of the so-prepared phases under oxidative conditions. These experiments are strongly connected to our previous studies on hydride formation on the corresponding Pd/SiO_2 catalysts [20], i.e. we further extended these studies to Pd supported on a variety of different oxidic materials, the first one being Al_2O_3. Secondly – as Pd–Al formation seems to have a major impact on the catalytic performance of Pd/Al_2O_3 catalysts – our goal is to make the Pd–Al interaction ''visible'' by means of utilizing transmission electron microscopy and selected area diffraction and to possibly identify distinct Pd–Al alloys. As already outlined in previous publications, we take advantage of the special properties of our thin film model systems, i.e. well-defined and ordered metal particles and a large contact area between metal and support [21].

2. Experimental

A high-vacuum chamber (base pressure 10^{-4} Pa) was utilized to prepare the Pd–Al_2O_3 thin films. Pd metal was deposited by electron-beam evaporation onto vacuum-cleaved, fresh NaCl(001) faces at a base pressure of around 10^{-4} Pa and a substrate temperature of 623 K. Under the chosen experimental conditions the deposition of Pd films of about 0.5 nm nominal thickness results in well-shaped Pd particles about 5–10 nm in size. Thereafter, the Pd particles were coated by a film of amorphous Al_2O_3 (nominal thickness 25 nm), prepared

by reactive deposition of Al metal in 10^{-2} Pa O_2 at room temperature. Subsequently, NaCl was removed by dissolution in distilled water, and, after careful rinsing, the resulting thin films were dried and mounted on gold grids for electron microscopy. To study the Pd–Al interaction and the structural and thermal stability of the resulting alloy phases, the films were subjected to reductive (1 bar H_2 for 1 h), oxidative (1 bar O_2 for 1 h) and annealing treatments (1 bar He for 1 h) in a circulating batch reactor in the temperature range 373–873 K. Transmission electron microscopy and selected area diffraction were used to monitor the structural and morphological changes occurring during the treatments. All the electron micrographs were taken with a Zeiss EM 10C microscope. The electron diffraction patterns were calibrated with respect to Pd reflections in the untreated, as-deposited Pd–Al_2O_3 state.

3. Results and discussion

3.1. *Pd–Al alloy formation upon annealing in He and reduction in H_2*

The initial state of the catalyst film after deposition is shown in figure 1a. The Pd particles are visible as dark and gray dots, respectively. Their average diameter was estimated by evaluating a number of TEM images from different parts of the sample to be around 8.5 nm. The dark ones are in almost perfect Bragg orientation while the gray ones are slightly tilted out of their respective Bragg position. Most of the particles exhibit rectangular or triangular shapes. Weak-beam dark field imaging revealed their cuboctahedral and tetrahedral habit [21]. In addition, also elongated and more rounded particles are sometimes encountered. It is also worth noting, that some very small Pd particles are visible, too. The SAED patterns (figure 1b) show intense Pd (200) and (220) reflections and a weaker (111) one (see table 1 for a detailed addressing of the measured lattice distances to the fcc Pd structure). Hence, most particles are oriented either along their [001] or [011] zone axis. The SAED patterns are corroborated by HRTEM images, showing mostly (200) Pd lattice spacings [21]. Thus, in most cases, the Pd particles expose a (100) plane to the electron beam. The Al_2O_3 support is usually amorphous in the as-deposited state and therefore does not contribute to the SAED patterns or exhibit a significant contrast in the TEM micrographs. It should however be noted, that Al_2O_3 readily crystallizes to γ -Al_2O_3 after a short time of illumination in an electron microscope.

Subsequently, the thin film was subjected to annealing treatments in He (1 bar for 1 h) at increasing temperatures to induce Pd–Al interaction. As it shown in figure 2a, the structure and the morphology of the Pd/Al_2O_3 film is not much altered if treated in He at 573 K and also the mean diameter of the particles did not increase very much. The SAED patterns (figure 2b) still only show reflections of the fcc Pd structure. The Pd spots, however, are slightly broadened, indicating a moderate increase of the orientational disorder of the Pd particles. First changes in the film structure are introduced upon raising the annealing temperature to about 723 K. Early stages of particle coalescence and a minor increase in the particle diameter are observed (figure 2c). This trend is also clearly visible in the corresponding SAED patterns (figure 2d). Apart from reflections of the Pd fcc structure, a number of new reflections at ~ 2.4 Å, ~ 2.16 Å, ~ 1.97 Å and ~ 1.55 Å are introduced. This indicates that during annealing at 723 K a phase transition has taken place and in fact, all of the newly appeared reflections are addressable to a cubic Pd_4Al_3 phase ($d_{theor}(200) = 2.410$ Å, $d_{theor}(210) = 2.156$ Å, $d_{theor}(211) = 1.967$ Å, $d_{theor}(310) = 1.524$ Å; lattice constant $a = 4.82$ Å, space group P213 [22]; see also table 1 for a complete listing of the measured lattice spacings). Further raising the annealing temperature to about 823 K does not change the structure of the film significantly and the Pd_4Al_3 alloy phase still persists.

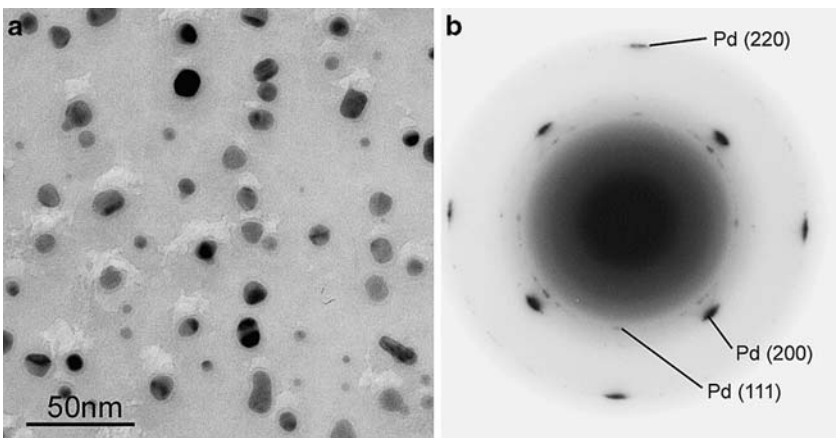

Figure 1. TEM micrograph of the as-deposited Pd/Al_2O_3 film (a) and its corresponding SAED pattern (b).

Table 1
Interplanar distances d(hkl) [Å] measured on the Pd/Al_2O_3 catalyst after different reductive and annealing treatments and possible correlation to fcc Pd, cubic Pd_4Al_3 and rhombohedral PdAl.

Pd/Al_2O_3 as-deposited			Pd/Al_2O_3 He 723 K			$Pd/Al_2O_3H_2$873 K		
$d(hkl)_{exp}$	Assignment		$d(hkl)_{exp}$	Assignment		$d(hkl)_{exp}$	Assignment	
	Lattice plane	$d(hkl)_{theor}$		Lattice plane	$d(hkl)_{theor}$		Lattice plane	$d(hkl)_{theor}$
2.25	Pd(111)	[2.245]	2.41	Pd_4Al_3 (200)	[2.410]	2.32	PdAl (21-2)	[2.338]
1.96	Pd(200)	[1.945]	2.26	Pd (111)	[2.245]	2.15	PdAl (250)	[2.176]
							PdAl (13-2)	[2.154]
1.39	Pd(220)	[1.375]	2.16	Pd_4Al_3 (210)	[2.156]	1.89	PdAl (502)	[1.888]
			1.97	Pd_4Al_3 (211)	[1.967]	1.80	PdAl (710)	[1.800]
							PdAl (51-2)	[1.787]
			1.93	Pd (200)	[1.945]	1.64	PdAl (45-1)	[1.652]
			1.55	Pd_4Al_3 (310)	[1.524]			

After annealing at the highest temperatures applied (873 K – figure 2e), the particles appear more rounded and have significantly increased in size compared to the as-grown state (average particle diameter around 11 nm), indicating a considerable mass transport, probably associated with alloy formation. It is worth noting, that no Pd reflections are visible in the SAED patterns, indicating that most of the former Pd has been transformed into the alloy state. The Al_2O_3 film shows first signs of structural reconstruction, indicated by the formation of characteristic "bubbles" [23]. However, no reflections of the fcc γ-Al_2O_3 are detectable in the diffraction patterns (figure 2f). Pd_4Al_3 reflections still persist, although their intensity decrease and blurring indicates that the stability limit of the alloy is reached, but according to the electron diffraction patterns even at the highest annealing temperatures only a single Pd_4Al_3 phase seems to be present.

In close correlation to experiments performed previously on Pd, Pt and Rh particles supported on reducible and non-reducible oxides [24–26] we also focused on the question if a metal-support interaction can also be triggered by reduction at elevated temperatures and if there are substantial differences to simple annealing treatments. Thus, the Pd/Al_2O_3 films were subjected to reductive treatments between 523 and 873 K in H_2 for 1 h each. Below 523 K reduction temperature, no structural or morphological changes were observable in the TEM images and the SAED patterns showed (partly disordered) Pd particles. At 523 K, the system transformed into the yet well-known amorphous hydride state [20]. Further raising the reduction temperature to 623 K destroys the amorphous state and new reflections appear at $\sim$ 2.32 Å, $\sim$ 2.15 Å, $\sim$ 1.89 Å, $\sim$ 1.80 Å and $\sim$ 1.64 Å. As a further raise of the reduction temperature to 873 K does not alter the electron diffraction pattern or the particle morphology, we show the pattern and TEM image obtained after reduction at the highest temperature (873 K) as a representative example (figure 3a, b). Although the SAED pattern appears to be similar to the one obtained in pure He at roughly the same temperatures, a careful analysis reveals the presence of a more Al-rich Pd alloy, namely PdAl. Hence, the reflections can be addressed to a rhombohedral PdAl phase (d_{theor}(21-2) = 2.338 Å; d_{theor}(250) = 2.176 Å; d_{theor}(13-2) = 2.154 Å; d_{theor}(502) = 1.888 Å; d_{theor}(710) = 1.800 Å; d_{theor}(51-2) = 1.787 Å; d_{theor}(45−1) = 1.652 Å; lattice constant a = 15.595 Å, c = 5.251 Å space group R-3) [27]. In contrast to the He experiments, it appears that the alloy formed in hydrogen is structurally more stable, as the SAED patterns still show very strong PdAl reflections after reduction at 873 K. The alloy formation also in this case goes along with a considerable increase in particle size (average particle diameter around 12.5 nm). The alumina support again shows typical signs of beginning reconstruction, although no reflections of crystallized alumina are detected in the SAED patterns.

Why do two different Pd–Al alloys most probably form upon annealing and reduction? We assume that structural differences do not play a dominant role, although the Pd_4Al_3 alloy crystallizes in a cubic lattice. The mismatch in the lattice constants of Pd and Pd_4Al_3 amounts to about 20% (3.89 Å versus 4.82 Å), which is much larger than e.g. between Pd and PdZn [28] and probably is too large to crucially influence the formation of Pd_4Al_3 and to induce a dominating topotactic growth of the alloy on top of the former Pd particles. We can, however, not fully neglect a possible "structural" influence. The same applies for the PdAl alloy, crystallizing in a rhombohedral lattice and bearing no crystallographic relationship with the fcc Pd lattice. It seems more plausible to discuss alloy formation in terms of a stepwise formation of Pd–Al alloys with increasing Al/Pd ratio depending on the annealing/reduction conditions. As we had already outlined previously, partial reduction of "non-reducible" oxides (e.g. SiO_2 or Al_2O_3) becomes feasible in thin film model catalysts at temperatures $T \geq 773$ K thereby mediating the formation of Pt-rich alloy compounds [24,25]. The first stages of alloy formation are believed to occur *via* a reduction of the oxide species and the subsequent migration of the

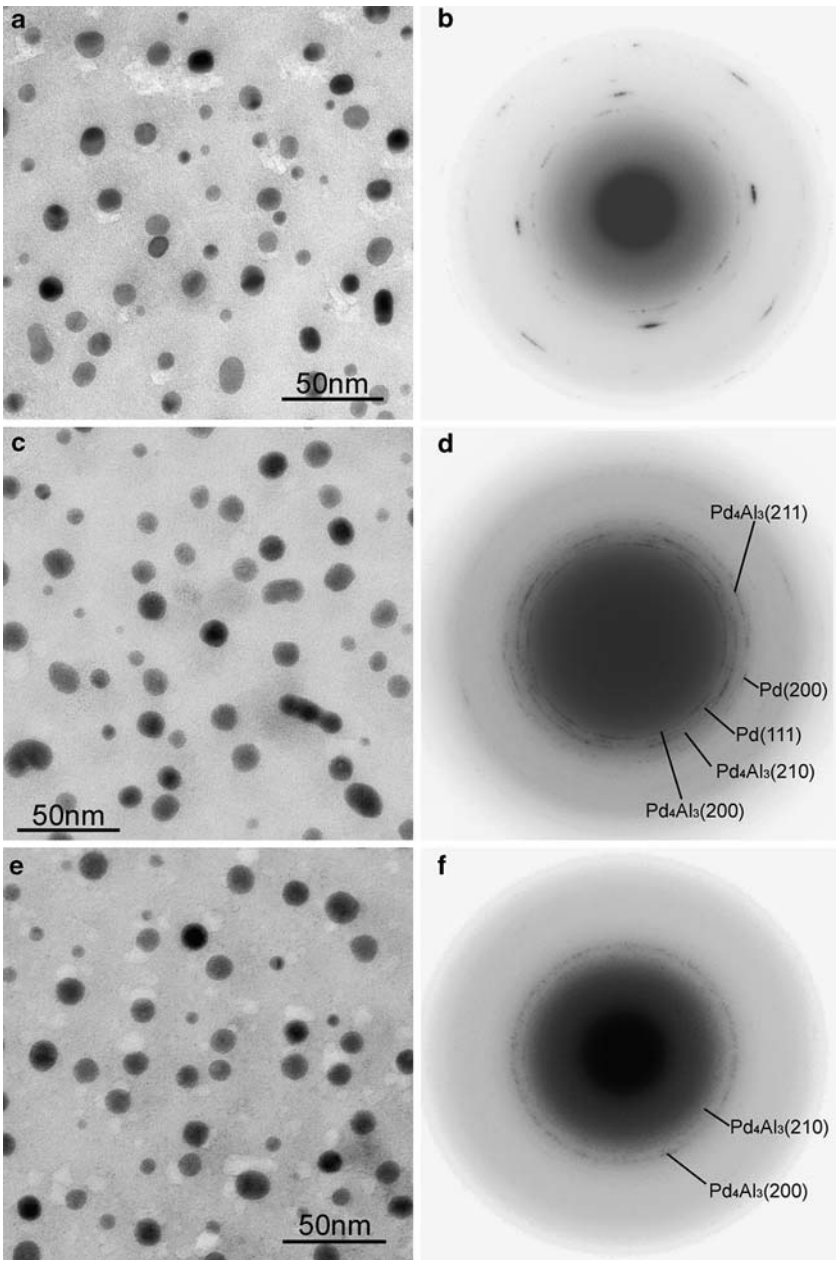

Figure 2. The Pd/Al_2O_3 film after different annealing treatments in 1 bar He for 1 h each. (a) 573 K, (c) 723 K and (e) 873 K. The corresponding SAED patterns are shown in (b), (d) and (f).

reduced species to the noble metal. Hence, it is plausible, that in the case of Pd/Al_2O_3 a relatively Pd-richer alloy forms at first upon annealing in He when the reduction of Al_2O_3 is not yet pronounced. Upon reduction in hydrogen, under otherwise comparable experimental conditions, the alumina support is more reduced compared to a simple annealing treatment, and hence, alloying is more pronounced and a relatively Al-richer alloy is formed (PdAl). A similar mechanism has also been observed for the Rh–V system, where the initial formation of Rh_3V has been followed by RhV at higher reduction temperatures (773 K) [29].

3.2. Stability of the alloy

In close correlation to similar experiments on Pd/SiO_2, we further tested the stability of the alloys under oxidative conditions. A second input for this measurement came from previous catalytic measurements, where the activity in alkane conversion upon different activative treatments has been correlated to compositional changes in the catalyst structure, namely the formation of a Pd–Al alloy at around 873 K. This alloy was found to decompose after an oxidative treatment and a subsequent low-temperature reduction

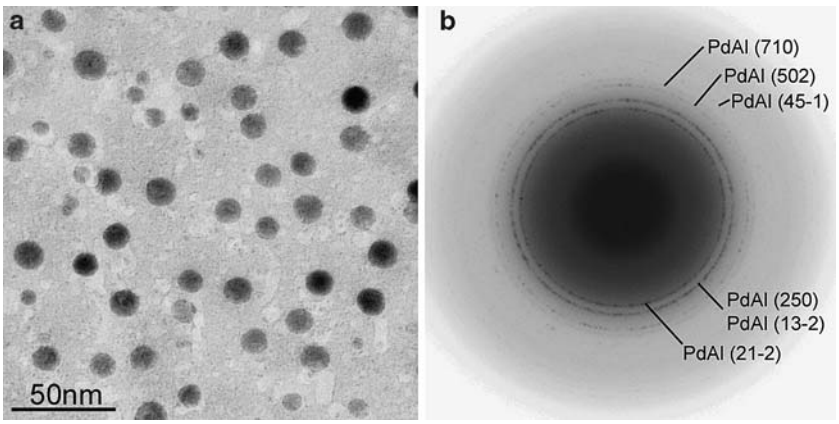

Figure 3. The Pd/Al_2O_3 thin film after a reduction in 1 bar H_2 at 873 K and its corresponding SAED pattern (b).

(473 K). Associated with these structural changes was a decrease in catalytic activity [10]. As we assigned alloy formation under comparable experimental conditions to two distinct Pd–Al alloys, it was interesting to see, if the stability limit of these alloys can also be correlated with these previous experiments. Therefore, both alloys were subjected to similar treatments at varying temperatures (up to 673 K) in 1 bar O_2 for 1 h each. The upper limit of 673 K was chosen because at this temperature, Pd particles are converted into a bulk PdO phase [30].

As it is clear from figure 4a (micrograph) and 4b (SAED pattern) the Pd_4Al_3 alloy still persists upon oxidation at 573 K. The mean diameter of the particles is almost unchanged and also the diffraction pattern only exhibits reflections of the Pd_4Al_3 structure. The situation changes if the oxidation temperature is raised to 673 K. Now the catalyst morphology much resembles

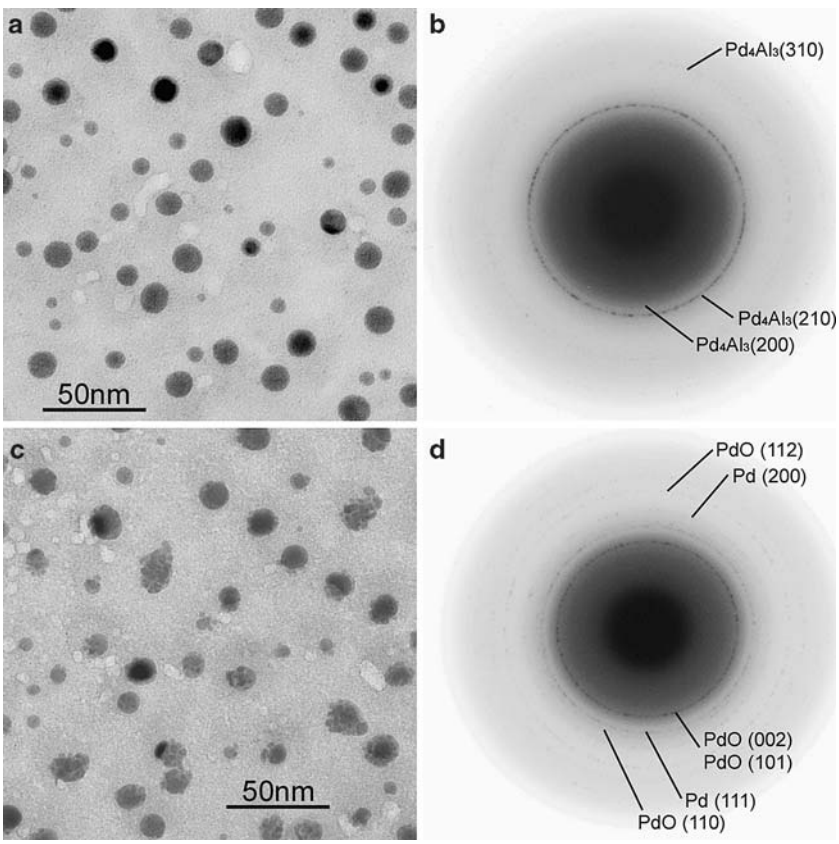

Figure 4. State of the Pd/Al_2O_3 film after a treatment in 1 bar He at 873 K followed by oxidation at 573 K (a) and 673 K (c). The SAED patterns are shown in (b) and (d).

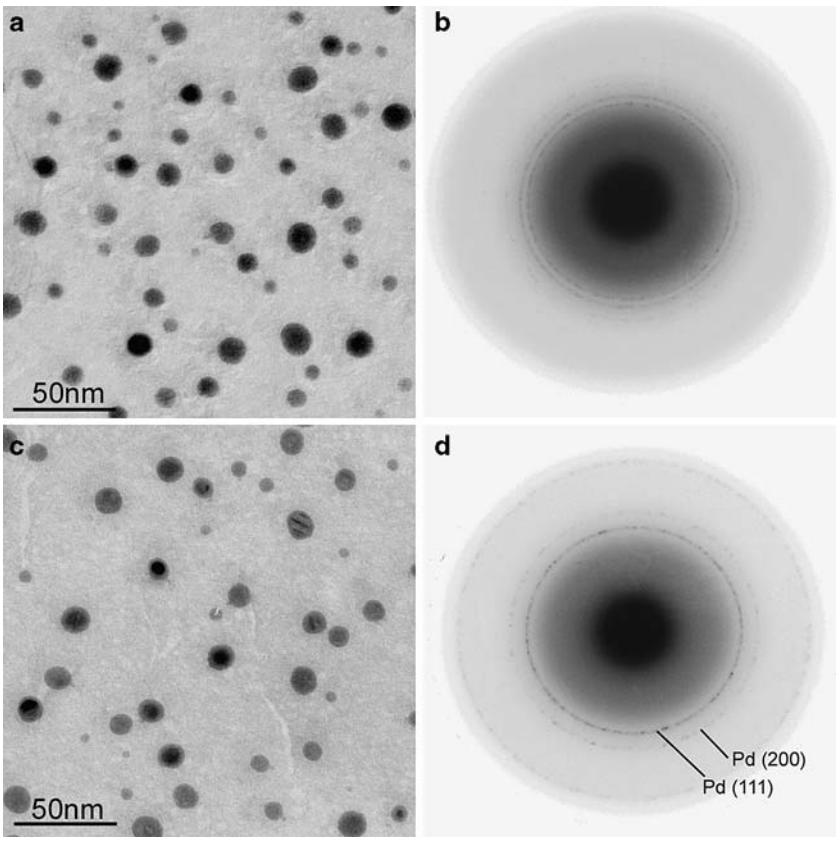

Figure 5. State of the Pd/Al_2O_3 film after a reduction in 1 bar H_2 at 873 K followed by oxidation at 523 K (a) and 623 K (c). The SAED patterns are shown in (b) and (d).

the one known from previous experiments on the oxidation of small Pd particles and exhibits the typical fragmented structure of PdO (figure 4c). Correspondingly, the SAED pattern only shows reflections of the tetragonal PdO phase (figure 4d) [30].

The PdAl alloy was also found to be stable under oxidative conditions up to 573 K. A representative TEM image (figure 5a) and a corresponding SAED pattern (figure 5b) taken after oxidation at 523 K are shown in figure 5. Further raising the oxidation temperature to 623 K, however, destroys the PdAl alloy and the SAED pattern only shows reflections arising from fcc Pd (figure 5d). TEM images reveal a slight decrease of the mean particle diameter (figure 5c). PdO is formed at oxidation temperatures above 623 K.

A question that remains to be answered is, if and how the hydride phase formed at reduction at 523 K can be transformed into a Pd–Al alloy by simple thermal annealing in He – as it was the case in the Pd/SiO_2 system. For this reason, we subjected a Pd/Al_2O_3 thin film to a reduction at 523 K and subsequently to an annealing treatment at 673 K in pure He. Figure 6a

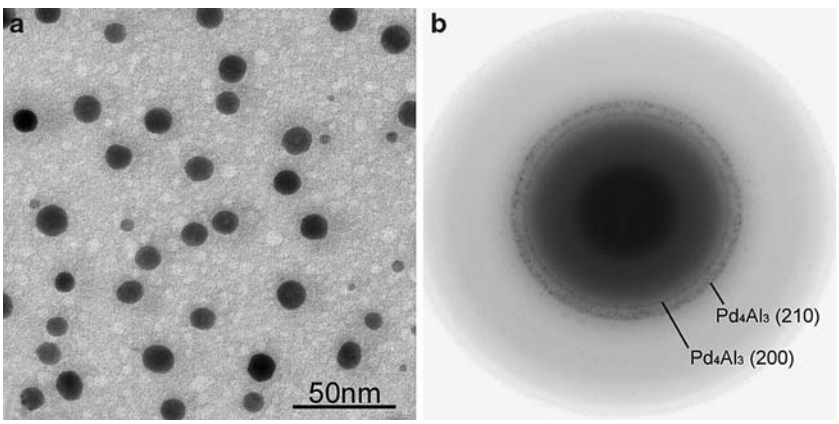

Figure 6. TEM image of the Pd/Al_2O_3 thin film after a reduction in 523 K in H_2 for 1 h followed by a treatment in He at 673 K (a). SAED pattern shown in (b).

(TEM micrograph) and 6b (SAED pattern) reveal that at this temperatures the amorphous hydride phase is destroyed and results in the formation of the Pd_4Al_3 alloy detected previously. A subsequent treatment in hydrogen does not transform the alloy back into the amorphous hydride phase (not shown here). Hence, as it was the case for Pd/SiO_2, the system loses its hydrogen storage capability upon entering an alloy state. A comparable effect has also been already observed in the Pd/Al_2O_3 system, where the formation of a Pd–Al alloy prevented the formation of a super-saturated Pd–C solid solution upon carburization in acetylene at 550 K [31].

3.3. Comparison to Pd–SiO_2

At this point it is useful to compare the results obtained on Pd/Al_2O_3 in more detail to those on Pd/SiO_2, as (i) Al_2O_3 and SiO_2 are both widely used as "non-reducible" supports for noble metal catalysts and (ii) one will gain more insight into the hydride stability as well as into the interaction of Pd with "non-reducible" oxide supports at elevated temperatures.

Hydride formation seems to occur on both systems at comparable temperatures. Hence, the active states of both catalysts in reactions involving H_2 consist either of a Pd-hydride phase and/or a hydride-induced heavily distorted Pd phase. In the case of Pd/Al_2O_3, this is especially interesting with respect to alkane hydroconversion after low-temperature reduction at $\sim$ 573 K. In addition, the amorphous (hydride) state is transformed into Pd–Si and Pd–Al alloys under comparable experimental conditions. It is, however, worth to note that in the Pd/SiO_2 film only one (Pd-rich) Pd_2Si alloy forms upon annealing and reduction. In contrast, two different alloys with different Al/Pd ratio form on Pd/Al_2O_3, depending on annealing or reduction. The stability limit of both Pd–Si and Pd–Al alloys in oxygen was found to be in the same temperature range, at about 573–623 K.

4. Conclusions

In close correlation to recent contributions and our own experiments on similar noble-metal-on oxide systems, Pd/Al_2O_3 thin films were found to be strongly affected by metal-support interaction, manifested as alloy formation at elevated temperature. A Pd-richer Pd_4Al_3 alloy has been identified after annealing treatments in He at temperatures above 673 K. In contrast, an Al-richer PdAl alloy has been observed after reduction in H_2 under otherwise similar experimental conditions. This structural difference was tentatively explained by a higher degree of reduction after a treatment in hydrogen and the subsequent formation of the relatively Al-richer alloy. Clear signs of beginning decomposition of the Pd_4Al_3 alloy have been observed at around 873 K annealing temperature, whereas the PdAl alloy seems to be stable at least up to 873 K. Under oxidative conditions, both Pd–Al alloys exhibit a similar stability and start to decompose in the temperature range 573–623 K. The above-presented results also imply that (i) the state of Pd/Al_2O_3 catalysts after a low-temperature reduction might be associated with a hydride and/or a highly distorted Pd phase (as it was the case for Pd/SiO_2) and (ii) that the use of the thin films model catalysts combined with electron microscopy techniques can be exploited to prepare and characterize distinct bulk Pd–Al phases with a higher Al/Pd ratio than reported previously on impregnated Pd/Al_2O_3 catalysts [10,31].

References

[1] S.M. Vesecky, D.R. Rainer and D.W. Goodman, J. Vac. Sci. Technol. A 14 (1996) 1457.
[2] M. Lyubovsky and L. Pfefferle, Appl. Catal. A 173 (1998) 107.
[3] M. Lyubovsky and L. Pfefferle, Catal. Today 47 (1999) 29.
[4] M. Lyubovsky, L. Pfefferle, A. Datye, J. Bravo and T. Nelson, J. Catal. 187 (1999) 275.
[5] R.J. Farrauto, M.C. Hobson, T. Kenelly and E.M. Waterman, Appl. Catal. A 81 (1992) 227.
[6] F. Le Normand, K. Kili and J.L. Schmitt, J. Catal. 139 (1993) 234.
[7] M. Skotak, D. Lomot and Z. Karpinski, Appl. Catal. A 229 (2002) 103.
[8] W. Juszczyk, D. Lomot, Z. Karpinski and J. Pielaszek, Catal. Lett. 31 (1995) 37.
[9] D. Lomot, W. Juszczyk and Z. Karpinski, Appl. Catal. A 155 (1997) 99.
[10] M. Skotak, Z. Karpinski, W. Juszczyk, J. Pielaszek, L. Kepinski, D.V. Kazachkin, V.I. Kovalchuk and J. Ld'Itri, J. Catal. 227 (2004) 11.
[11] S.J. Fauster, S.C. Fung and R.L. Garten, J. Am. Chem. Soc. 100 (1978) 170.
[12] I. Matolinova, V. Johanek, T. Skala, K. Veltruska and V. Matolin, Appl. Surf. Sci. 245 (2005) 87.
[13] V. Johanek, N. Tsud, V. Matolin and I. Stara, Vacuum 63 (2001) 15.
[14] L.Q. Jiang, M.W. Ruckman and M. Strongin, Phys. Rev. B 39 (1989) 1564.
[15] S. Nemsak, K. Masek and V. Matolin, Vacuum 80 (2005) 102.
[16] V. Shutthanandan, A.A. Saleh, N.R. Shivaparan and R.J. Smith, Surf. Sci. 350 (1996) 11.
[17] V. Johanek, I. Stara and V. Matolin, Surf. Sci. 507–510 (2002) 92.
[18] B. Frick and K. Jacobi, Phys. Rev. B 37 (1989) 4408.
[19] J.J. Chen and E. Ruckenstein, J. Catal. 69 (1981) 254.
[20] B. Jenewein, S. Penner, H. Gabasch, B. Klötzer, D. Wang, A. Knop-Gericke, R. Schlögl and K. Hayek, J. Catal. 24 (2006) 155.
[21] G. Rupprechter, K. Hayek, L. Rendon and J.-M. Yacaman, Thin Solid Films 260 (1995) 148.
[22] Powder Diffraction File 1994, PDF 2 Database 1-44, International Center for Diffraction Data, Geneva7, pattern # 00-029-0066 and references therein.
[23] G. Rupprechter, PhD-thesis, University of Innsbruck, 1995.
[24] S. Penner, D. Wang, D.S. Su, G. Rupprechter, R. Schlögl and K. Hayek, Surf. Sci. 532–535 (2003) 276.
[25] S. Penner, G. Rupprechter, H. Sauer, D.S. Su, R. Tessadri, R. Podloucky, R. Schlögl and K. Hayek, Vacuum 71 (2003) 71.
[26] S. Penner, D. Wang, R. Schloegl and K. Hayek, Phys. Chem. Chem. Phys. 6 (2004) 5244.
[27] T. Matkovic and K. Schubert, J. Less-Common Met. 55 (1977) 45; Powder Diffraction File 1994, PDF 2 Database 1-44,

International Center for Diffraction Data, Geneva7, pattern # 01-071-5919.
[28] S. Penner, B. Jenewein, H. Gabasch, B. Klötzer, D. Wang, A. Knop-Gericke, R. Schlögl and K. Hayek, J. Catal. 241 (2006) 14.
[29] S. Penner, B. Jenewein, D. Wang, R. Schlögl and K. Hayek, Phys. Chem. Chem. Phys 8 (2006) 1223.
[30] S. Penner, D. Wang, B. Jenewein, H. Gabasch, B. Klötzer, A. Knop-Gericke, R. Schlögl and K. Hayek, J. Chem. Phys. (in press).
[31] L. Kepinski, M. Wolcyrz and J.M. Jablonski, Appl. Catal. 54 (1989) 267.